Glass Transition Behavior of a Microphase Segregated Polyurethane Based on PFPE and IPDI. A Calorimetric Study

Mattia Bassi,* Claudio Tonelli, and Antonella Di Meo

Solvay-Solexis R&D Center, Viale Lombardia 20, I-20021 Bollate, MI, Italy

Received May 21, 2003

ABSTRACT: A series of segmented polyurethanes obtained from perfluoropolyether (PFPE) and isophorone diisocyanate (IPDI) were studied by using quantitative thermal analysis. The glass transition behavior of the segregated phases of the segmented copolymers, compared to the corresponding amorphous homopolymers, was characterized in order to determine the dependence of the phase separation on the composition. The glass transition was observed to shift and broaden for both the hydrogenated and the fluorinated phase, reducing the corresponding content in the polymer, and the measured Δc_p on the segregated phases deviates from the expected ones according to the homopolymer values. To investigate the effects of the size of the separated domains and of the interfacial constraints on the glass transition behavior, heat capacity measurements were carried out on PFPE models with perfluorinated or methilolic chain ends absorbed on amorphous silica. The chain mobility reduction associated with a nanoscopic confinement is responsible for the effects on the glass transition measured by DSC. This phenomenon seems to rule the observed similar behavior within the polyurethane series investigated in the present work.

Introduction

The properties of linear segmented polyurethanes of the $(S-H)_n$ type, where S and H are thermodynamically incompatible soft and hard segments, are related mainly to the structure deriving from phase separation.[1−3]

Consequently, in the recent literature a number of studies are devoted to the characterizing methodologies for the degree of microphase separation, in terms of either dimension or composition of the separated domains.[4−12]

Differential scanning calorimetry (DSC) is perhaps the most widely used tool due to its relative simplicity and to the possibility of quantitative measurements. On the grounds of the comparisons of measured glass transition temperature (T_g) and change of heat capacity at the transition (Δc_p) of the copolymer phases to the values of the pure hard and soft segments, many relationships[4−8] have been proposed in order to calculate the degree of the microphase separation.

However, these analytical methods often brought to controversial or inconclusive results due to the lack of reliable models for the amorphous hard phase (T_{g_H} and Δc_{p_H}). In fact, hard segments were reported to partially crystallize and assemble in domains with different degrees of order, as demonstrated by multiple melting endotherms,[9−11] and the hard amorphous phase was not univocally characterized. As a matter of fact, the assumption of $\Delta c_{p_H} = 0$ has been often employed.[6,7]

In a recent paper,[12] performing a calorimetric analysis of a series of completely mixed polyurethanes, a Δc_{p_H} value for the hard phase consistent with the measured value on the high molecular weight homopolymer $(H)_n$ was determined. However, the same work highlighted the difficulty of the application of the obtained value for a quantitative study on an analogue phase-separated series owing to microdomain morphology and molecular weight effects on the measured heat capacity change of the segregated segments.

* Corresponding author: e-mail mattia.bassi@solvay.com.

Recent contributions have shown that the introduction, in a semicrystalline polymeric matrix, of a soft block of perfluorinated polyether (PFPE), characterized by a very low solubility parameter δ (10.5 $J^{1/2}/cm^{3/2}$),[13] enhances the thermodynamic incompatibility with the urethane hard block. A new class of materials with unique properties related to the presence of a segregated fluorinated phase at the solid/air interface has been so developed.[14−16]

The structures investigated in the present work differ from the already described systems because they are obtained by two amorphous components with a substantially different solubility parameter, which is an effective driving force to efficiently promote a phase segregation also for very low molecular segments. The hydrogenated segment of the present polyurethane series is constituted by just one diisocyanate molecule without any chain extender connecting two or more diisocyanate units. This structure, based on the available literature data, should not give a phase separation; in fact, very short hard segments, i.e., diisocyanate coupled with two soft segments, are reported to be included in a mixed phase with the soft component.[17] On the contrary, the polyurethane series of the present study are segregated segmented polymers, whose homopolymer glass transition temperatures differ by more than 200 deg. They should represent good models for a study of size and constraints effects on segregated phases by thermal analysis.

Experimental Section

Materials. Six diolic perfluoropolyethers (Fomblin ZDOL by Solvay Solexis) with a molecular weight ranging between 522 and 4705 have been used as macromonomers for the synthesis of segmented polymers. Their structure is reported in Chart 1; their main molecular characteristics are reported elsewhere[9] and summarized in Table 1.

A further ZDOL sample of molecular weight of 1069, named ZDOL HF, has been used to elucidate interfacial effects on the chain mobility and calorimetric characteristics. This has been achieved by absorbing this fluorinated diol on silica gel

10.1021/ma034674g CCC: $25.00
Published on Web 09/16/2003

Chart 1. Structures of the Fluorinated Macromonomers ZDOL, Fomblin Z, and the Polyurethanes ZDOLI[a]

$HOCH_2CF_2(OCF_2)_q(OCF_2CF_2)_pOCF_2CH_2OH$ (1) ZDOL

$XCF_2(OCF_2)_q(OCF_2CF_2)_pOCF_2X'$ (2) Fomblin Z

(where X, X' = Cl, F, CF_2Cl,)

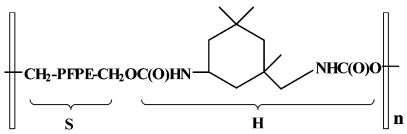

(3) ZDOLI

[a] PFPE represents the perfluoropolyetheric chain $-CF_2(OCF_2)_q(OCF_2CF_2)_pOCF_2-$.

Table 1. Characteristics of Fluorinated Macromonomers

sample	M_n (NMR) (g/mol)	M_n (GPC) (g/mol)	M_w/M_n (GPC)	p/q	functionality
ZDOL-1	522	560	1.1	1.31	1.99
ZDOL-2	950	990	1.1	0.95	1.97
ZDOL-3	1214	1280	1.2	1.26	1.98
ZDOL-4	2194	2280	1.4	0.88	1.97
ZDOL-5	3573	3470	1.2	1.20	1.96
ZDOL-6	4705	4180	1.1	1.19	1.96
ZDOL-HF	1069	1038	1.1	0.90	1.99
Fomblin Z	3176			0.94	

and comparing the absorption effect with that observed for an unfuctionalized perfluoropolyether macromonomer (Fomblin Z by Solvay Solexis) whose structure (Chart 1) can be assumed as a model for the soft fluorinated phase. Their main structural properties are reported on the bottom of Table 1.

Poly(ethylene glycol-*co*-isophorone diisocyanate) has been synthesized as a model of the hard hydrogenated phase.

Isophorone diisocyanate (IPDI), ethylene glycol, and dibutyltin dilaurate (DBTDL), all from Aldrich, were used as received. Ethyl acetate and methyl ethyl ketone (MEK), from Aldrich, were distilled just before use.

Silica gel 60 (from Fluka), ≤230 mesh, was used as received.

Synthesis of Polyurethanes. The polyurethane samples (ZDOLI) with a segmented block copolymeric structure $(S-H)_n$ (structure **3** in Chart 1) where S and H indicate the soft and the hard segment, respectively, were prepared by the bulk polymerization process described below:

ZDOL (263 mequiv) was charged into a reactor and heated at 330 K. The catalyst DBTDL (0.01% with respect to the hydroxyl equivalent) was added together with IPDI (263 mequiv). The reaction mass was vigorously stirred and degassed under vacuum for 5 min. The mass was cast into a mold and placed in a press to complete the polymerization (from 350 to 400 K within 30 min and 24 h at 400 K).

The reaction kinetic was monitored by IR analysis observing the disappearance of the typical isocyanate absorption band (2260 cm^{-1}).

All samples were conditioned for at least 2 weeks at room temperature before testing.

Synthesis of Poly(ethylene glycol-*co*-isophorone diisocyanate) (IPG). The polymeric hard model has been prepared by a one-step solvent polymerization procedure. Ethylene glycol (2 g, 64 mequiv) and 75 mL of freshly distilled ethyl acetate were charged into a reactor under inert atmosphere. 7.5 g of IPDI (68 mequiv) was added under stirring together with 1.1 mL of DBTDL dissolved in MEK (20% w/w solution, DBTDL 1% on a molar base with respect to the IPDI). The reaction mass was heated to the solvent reflux condition (350 K). The reaction mass was vigorously stirred for 6 h, until the IR analysis confirmed the complete −NCO consumption. Finally, the solvent was removed by vacuum distillation. A white solid powder was isolated (9.5 g).

Preparation of Silica Blends. Two series of four samples have been prepared by absorption of a proper amount of ZDOL-HF or Fomblin Z on silica gel by the following procedure. A 9−10% (w/w) solution of the fluorinated compound in CFC 113 was added dropwise to a silica dispersion in the same solvent (11% w/w) at room temperature. The resulting slurry was stirred for 2 h in order to reach equilibrium composition. Finally, the solvent was removed by vacuum distillation and the dry solid isolated.

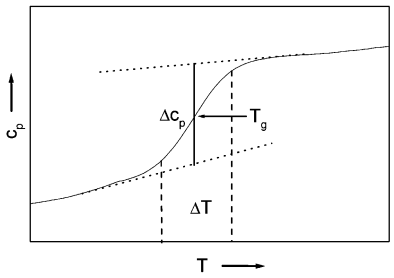

Figure 1. Definitions of the glass transition parameters from a heat capacity vs temperature curve. Data from sample ZDOLI-4 in the low glass transition region.

NMR Spectroscopy. ^{19}F NMR spectra were recorded on neat samples using a Varian Mercury instrument operating at 288 MHz. This technique was used to determine the molecular parameters of ZDOL samples (number-average molecular weight M_n, composition of the chain, i.e., the molar fraction of $-CF_2O-$ and $-CF_2CF_2O-$ repeating units and functionality). The results obtained by this technique are well consistent with complementary information acquired by GPC analysis.

GPC Analysis. The molecular weight characterization of ZDOL macromonomers by GPC analysis was carried out by means of a Waters model 5900 GPC instrument, equipped with four "Ultrastyragel" columns of 10^5, 10^4, 10^3, and 500 Å porosity at 310 K using 1,3-bis(trifluoromethyl)benzene as eluent. The calibration curve was obtained with narrow MWD ZDOL fractions whose M_n was determined by ^{19}F NMR analysis.

Density. Because of their waxy characteristics, the density of ZDOLI-2−6 was determined coating PTFE thin films of measured weight and density with a similar weight of sample, while ZDOLI-1 and IPG were directly compression molded. Densities were determined weighting the samples in air and in water at 296 K according to ASTM D792: measurements were repeated three times, and the reproducibility was within 1%.

Heat Capacities. Calorimetric measurements were carried out by means of a Perkin-Elmer DSC2 equipped with a refrigeration unit with liquid nitrogen for controlled cooling to 110 K and a drybox fluxed with a nitrogen gas purge in order to prevent any frost accumulation on the calorimetric head. The customary three-step procedure[18] (baseline run, sample run, and standard Al_2O_3 run) was followed to determine heat capacity data. The whole thermal range (from 120 to 320 K), calibrated with reagent grade *n*-hexane, *p*-nitrotoluene, and indium, was split into four separated steps. The scan rate was 10 K/min. To achieve the better baseline linearity and stability, the standard helium flux was substituted by a neon flux for $T > 223$ K.

The cooling rate was set at 5 K/min, and all the scans were repeated on a different set of samples. Differences in heat capacity values between the two set of samples were always less than 4%. Simple DSC scans (without Al_2O_3 calibration) were also collected after cooling at 80 K/min, which is the maximum controlled cooling rate instrumentally allowed in the temperature range.

T_g was determined as the fictive temperature, defined by the intersection of the extrapolated pre-transition and post-transition enthalpy data (obtained by the integration of the heat capacity curve).[18] Figure 1 shows the definitions of the other parameters of a glass transition obtained from the c_p vs T curves. The heat capacity step Δc_p was calculated as the distance between the extrapolated linear heat capacity below and above the transition lines at T_g; the glass transition width

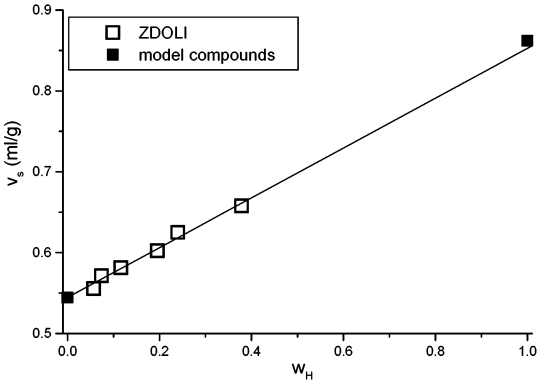

Figure 2. Specific volume of ZDOLI series and of the model compounds. The line is the linear fit of the ZDOLI data.

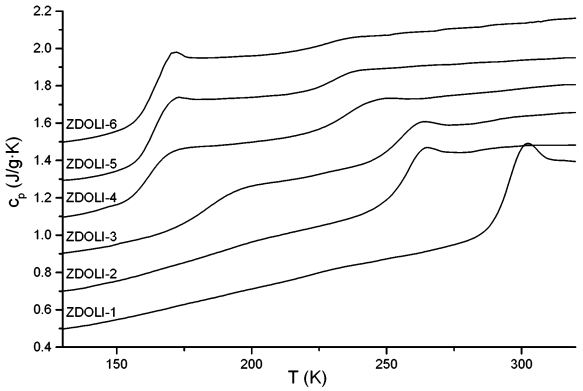

Figure 3. Heat capacity of the ZDOLI series, after cooling at 5 K/min. The *Y* axis corresponds to data on ZDOLI-1 only. Subsequent curves have been shifted successively by 0.2 J/(g K).

ΔT was the temperature interval intercepted by the projection on the T scale of the experimental values corresponding to 16% and 84% of the total Δc_p step.

To check the reliability of the obtained results, measurements on sample ZDOLI-1 and on silica based blends have been repeated on a Perkin-Elmer Pyris 1 calorimeter, claimed to profit by a shorter time constant and a higher resolution in the determination of weak transitions. No substantial differences have been detected, and the obtained parameters agree with previous results within a 5% uncertainty.

Results and Discussion

Specific Volume. Figure 2 shows the specific volumes of the copolymer series represented as a function of the weight fraction of the hydrogenated segments w_H. The observed linear trend extrapolates, at a vanishing hydrogenated content, to a value (0.545 cm^3/g) which compares well with that found for unfunctionalized PFPE of the same structure (0.547 cm^3/g).[19]

Considering the measured value of the hard phase model IPG (0.862 cm^3/g) as the upper limiting value, specific volumes follow an additivity rule with a maximum spread of 2%.

However, it must be considered that at the temperature at which density measurements are carried out (296 K) the model IPG is solid, while the whole copolymeric series is in the liquid state.

Assuming an ordinary behavior for the specific volume of IPG at transition ($v_{liquid} > v_{solid}$), the samples of these series, analogous to other end-capped PFPE macromonomers[9,20] show a weak loss of volume by increasing the hydrogenated content. These phenomena are consistent with other evidence, like T_g values higher than the corresponding values on the unfunctionalized PFPEs.[19,21]

This unusual behavior is magnified when low molecular weight end-capped macromonomers are considered as a consequence of the cohesive contribution of the hydrogenated polar segments in the liquid state.[9,12]

DSC Analysis. Heat capacities for the ZDOLI series are shown in Figure 3, and the related calorimetric data are reported in Table 2. Calorimetric traces indicate that all materials are amorphous and biphasic. c_p measurements have been preferred to the usual baseline method because of the inherent better correctness of the quantitative evaluations. The actual knowledge of heat capacity as a function of temperature before, after, and between the transitions allows either a more reproducible determination of T_g's parameters or the possibility of a check on c_p additivity for the whole series of copolymers. The knowledge of the thermal behavior of transitions spread over hundreds of degrees is hardly accessible by a standard thermal run on a commercial power compensation calorimeter, also with the most careful check on baseline stability.

To verify the kinetic dependence of the phase separation process, the cooling rate has been varied from 5 to 80 K/min, i.e., the maximum cooling rate instrumentally allowed for the temperature range of analysis. Differences in the measured T_g's are always less than 4 K, and also Δc_p and ΔT never exceed 20%. These results are probably due to the strong incompatibility between the hydrogenated and fluorinated moieties also in the liquid state, so that kinetic effects do not substantially affect the phase formation and segregation process. As a matter of fact, differences at various cooling rates are hardly envisaged also in phase-separating end-capped perfluoropolyether macromonomers[9] as well as in Fomblin Z, which is considered as a model for the soft chain.[22]

Hysteresis effects could be helpful in detecting weak thermal events. However, the areas under the endothermic peaks due to enthalpy relaxation have been reported to be strongly reduced in block copolymers, although phase segregated,[23,24] compared to homopolymers. A strong reduction of the hysteresis behavior has been observed also in semicrystalline polymers[25,26] and in blends[27] and has been generally associated with the broadening of the glass transition.[28] In the segmented copolymers which are object of this study, hysteresis peaks are detectable only in proximity of hard transitions of the first samples of the series (ZDOLI-1 and ZDOLI-2) and of the soft transitions of the higher samples (ZDOLI-4−6).

T_g values of both hard and soft phases have an almost linear dependence on hydrogenated phase weight fraction w_H, as shown in Figure 4.

Analogous to the precursor ZDOL and other derived biphasic structures previously examined,[9] T_g of the soft fluorinated phase extrapolates to a value (147 K) close to that of the model PFPE with unfunctionalized chain ends (Fomblin Z, structure 2). Moreover, it should be noted that T_g values of the samples with higher content of soft phase (ZDOLI 4−6) are quite similar to those found for ZDOL of equal molecular weight,[9] suggesting the formation of a completely segregated fluorinated phase. In fact, because of the large differences in the solubility parameters, the hydrogenated phase is "ejected" from the vitrifying fluorinated also at a very low hard phase contents.

Table 2. Glass Transition Behavior[a] of the Series ZDOLI and of the Model Compounds[b]

sample	w_H[c]	$T_{g_{SP}}$ (K)	$\Delta c_{p_{SP}}$ (J/(g K))	ΔT_{SP} (K)	$T_{g_{HP}}$ (K)	$\Delta c_{p_{HP}}$ (J/(g K))	ΔT_{HP} (K)
IPG	1				357 ± 1.5	0.497 ± 0.011	12 ± 2
ZDOLI-1	0.380	219.6 ± 3.5	0.020 ± 0.013	26 ± 3	290.9 ± 2	0.351 ± 0.005	15 ± 3
ZDOLI-2	0.239	180.1 ± 2	0.064 ± 0.005	32 ± 5	254.1 ± 1	0.219 ± 0.006	16 ± 2
ZDOLI-3	0.197	182.7 ± 0.8	0.129 ± 0.007	24 ± 4	249.8 ± 1	0.149 ± 0.006	19 ± 3
ZDOLI-4	0.116	160.8 ± 1.2	0.209 ± 0.011	17 ± 2	230.1 ± 2.5	0.124 ± 0.014	21 ± 5
ZDOLI-5	0.074	162.2 ± 0.8	0.270 ± 0.008	9.5 ± 2	228.6 ± 3	0.089 ± 0.008	25 ± 4
ZDOLI-6	0.057	160.6 ± 0.9	0.286 ± 0.009	8 ± 2	224.5 ± 4	0.050 ± 0.007	26 ± 4
Fomblin Z	0	147.1 ± 0.6	0.293 ± 0.008	4 ± 1			
ZDOL-HF	0.051	173.4 ± 0.9	0.305 ± 0.010	7 ± 2			

[a] After cooling at 5 K/min. [b] Reported errors are mean deviations. [c] Hydrogenated weight content.

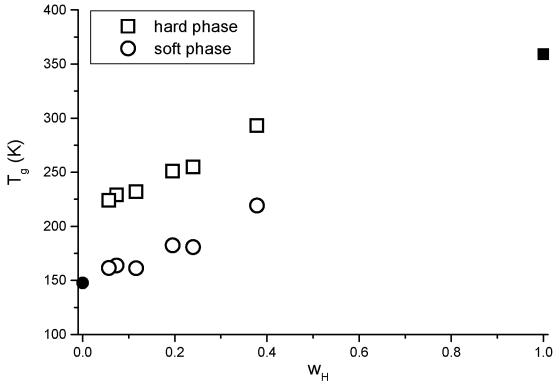

Figure 4. T_g of the hard (□) and soft (○) phases vs the weight fraction of the hydrogenated moieties. Solid markers refer to soft and hard models.

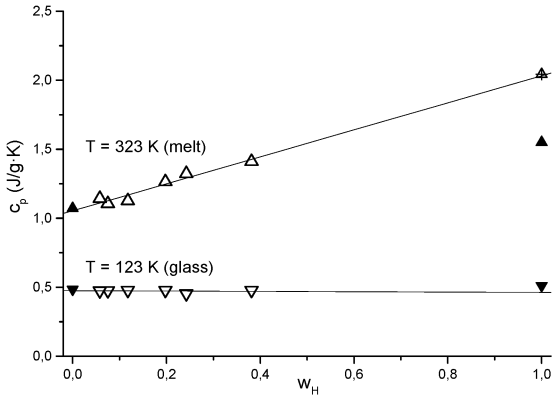

Figure 5. Heat capacity of the series vs the weight fraction of the hydrogenated moieties in the glassy state (123 K, below T_g of the soft segment, ▽) and in the molten phase (323 K, above T_g of the hard phase, △). Solid symbols are hard and soft models measured at 123 and 323 K; the crossed triangle is the heat capacity of the hard model IPG at 323 K corrected by the heat capacity step at T_g (see text).

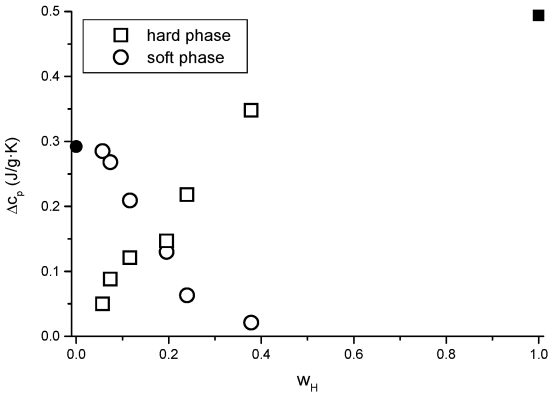

Figure 6. Measured Δc_p for the fluorinated (○) and hydrogenated (□) phases vs the weight fraction of the hydrogenated moieties. Solid symbols are Δc_p of hard and soft models.

On the other side, the hard phase shows an increasing glass transition temperature when decreasing molecular weight of the fluorinated part, demonstrating that also very short soft segment lengths do promote the formation of mixed phases. The extrapolation at $w_H = 1$ gives a T_g of 417 K, which is surprisingly high when compared to the measured T_{g_H} (357 K) of the hard polymeric model (IPG).

More generally, in block copolymers of even partially compatible segments, generation of mixed phases is proved by the tendency of the glass transition of hard and soft domains to converge toward a common temperature.[24,29,30] Therefore, the almost identical, positive slope of the interpolating lines of both phases' T_g found in the studied series accounts for a complete segregation in the full composition range.

However, the simple analysis of the behavior of the glass transition temperatures is unable to clarify the actual nature of the system under investigation. It is well-known that transitions of an inhomogeneous, amorphous material could be affected, besides by composition, by phase constraints,[24] crystallinity,[31] cross-linking,[32] and phase size effects.[12,23,33]

To obtain a more quantitative evaluation of the actual phase separation of the system, heat capacity data should be examined. Figure 5 shows the experimental heat capacity of the series compared to values obtained on the soft model (Fomblin Z) and on the hard one (IPG). The hard model at 323 K is a solid ($T_{g_H} = 357$ K), so the measured value is reasonably lower than the extrapolated one in a completely molten series. The crossed square in Figure 5 is calculated summing up to the experimental heat capacity the step corresponding to the glass transition ($\Delta c_{p_H} = 0.497$ J/(g K)): this value agrees with the extrapolated one within 2%.

The additivity of the two blocks heat capacity both in the glassy and in the liquid state is demonstrated by linear regressions (solid lines in Figure 5). The minor fluctuation can be ascribed to variation in the p/q ratio in the fluorinated segment of different samples.[22]

As a consequence, the overall increase in heat capacity from the glassy to the liquid state is a function only of the composition. On account of this statement, Δc_p measurements should be a useful, and actually quantitative, tool for the determination of the size and the composition of the separated phases.

Figure 6 shows the measured Δc_p for both soft and hard phase transitions. While the hydrogenated phase extrapolates to 0 at $w_H = 0$, the soft transition seems to disappear at a fluorinated phase content below 60%. On the other side, while at zero hydrogen content fluorinated phase extrapolates not far from the expected

value (0.293 J/(g K), the measured value of the soft model), the hydrogenated one gives, at $w_H = 1$, a larger value than expected as indicated by the hard model ($\Delta c_{p_H} = 0.497$ J/(g K)).

In accordance with the linear relationships introduced in the literature,[4−7] on the basis of a simple additive hypothesis, it is possible to evaluate the effectiveness of the phase separation defining a segregation ratio for the soft and the hard phases as follows:

$$R_H = \Delta c_{p_{HP}}/(w_{HH}\Delta c_{p_H} + (1 - w_{HH})\Delta c_{p_S}) \quad (1)$$

$$R_S = \Delta c_{p_{SP}}/(w_{SS}\Delta c_{p_S} + (1 - w_{SS})\Delta c_{p_H}) \quad (2)$$

where $\Delta c_{p_{SP}}$ and $\Delta c_{p_{HP}}$ are the observed change in specific heat of the soft and hard phase, Δc_{p_S} and Δc_{p_H} are the heat capacity change of the pure components, and w_{SS} and w_{HH} are the weight fraction of the soft fraction in the soft phase and the weight fraction of the hard segment in the hard phase, respectively.

In the polyurethanes literature, the R_S ratio, elsewhere indicated as segregation rate[7] or segregation degree,[35] is often reported; however, its use is frequently simplified, neglecting the heat capacity contribution of the hard component Δc_{p_H}.[6,7] In our completely amorphous copolymers series, Δc_{p_H} and Δc_{p_S} are comparable, so that this simplification is no longer true. Therefore, the quantitative evaluation of two transitions, even if clearly separated, cannot lead to a univocal picture of the phase composition.

Considering for instance the high-temperature transitions, a picture in which lowering the molecular weight of the fluorinated component an increasing content of soft segments is confined in the glassifying hydrogenated phase, seems to be supported by the measured increase in Δc_{p_H}. These findings are apparently in accordance with previous outcomes on similar systems[9,34] reporting the complete segregation of the fluorinated phase only for molecular weights higher than 1000, whereas shorter chains lead to less efficient segregation. However, the observed concurrent increase, in the present series, of the measured $T_{g_{HP}}$ clearly contradicts this interpretation.

An additional problem arises from the significance, in eqs 1 and 2, of the comparison of heat capacity steps measured at different T_g. In a vitrifying material, Δc_p is the jump between liquid and glassy heat capacity characterizing the iso-entropical transition associated with cooperative freezing-on of long-range motions.

Assuming a linear behavior for the heat capacity both in the glassy region just under T_g and in the liquid phase just above T_g, the dependence of Δc_p from the temperature of the transition can be written as follows:

$$\Delta c_p(T_{g_{obs}}) = \Delta c_p(T_g) + (dc_p^{liq}/dT - dc_p^{gl}/dT)(T_g - T_{g_{obs}}) \quad (3)$$

Because of the additivity of experimental heat capacities in both liquid and glassy states, eq 3, graphically illustrated in Figure 7, can be applied to the studied series. (Incidentally, we can observe that similar results could be obtained by means of the Sihma−Boyer empirical rule, $T_g\Delta c_p = \text{cost.}$)

Introducing the "corrected" experimental values in eqs 1 and 2 and the Δc_{p_H} and Δc_{p_S} measured on the model samples ($\Delta c_{p_H} = 0.497$ J/(g K) and $\Delta c_{p_S} = 0.293$ J/(g K)),

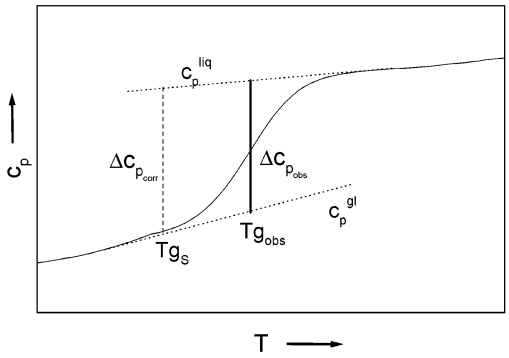

Figure 7. Graphical illustration of the dependence of Δc_p on the glass transition temperature. Data from sample ZDOLI-4 in the low glass transition region.

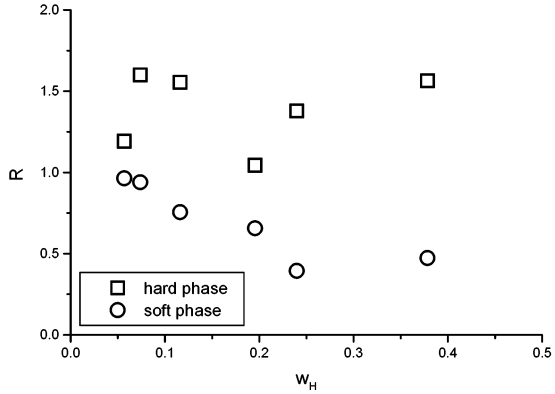

Figure 8. Segregation ratio of the soft phase R_S (○) and of the hard phase R_H (□) vs the weight fraction of the hydrogenated moieties. The ratios are calculated assuming an homophasic composition for both the hard and soft domains (see text).

the ratios R_H and R_S, could be calculated only with an arbitrary hypothesis on the composition of the separated phases. Assuming that the complete incompatibility between hydrogenated and fluorinated moieties generates homophasic domains (w_{HH} and $w_{SS} = 1$), the ratios are plotted as a function of the hydrogenated content w_H in Figure 8.

While hard phase data are scattered without a univocal trend round a value greater than the unit, probably due to the uncertainty in the assumption of the model Δc_{p_H}, the soft phase segregation ratio clearly shows a decrease with lowering the fluorinated segment length.

A final insight into the nature of the separated phases could be gained from the analysis of the width of the transitions. The glass transition of the fluorinated phase is broadened when molecular weight of the soft segment is decreased. The hard transition shows a similar trend: the higher the hydrogenated content, the sharper the associated glass transition.

Donth[36,37] proposed the association of the transition width, measured by DSC, to a characteristic length ξ_r, defined as the cube root of the mean volume V_r of the cooperatively rearranging regions (CRR).

$$V_r = \xi_r^3 = k_B T^2 \Delta(1/c_v)/(\rho \delta T^2) \quad (4)$$

where $\Delta(1/c_v)$ is the step height of reciprocal heat capacity at constant volume, ρ the density, and δT the average temperature fluctuation of a CRR. According

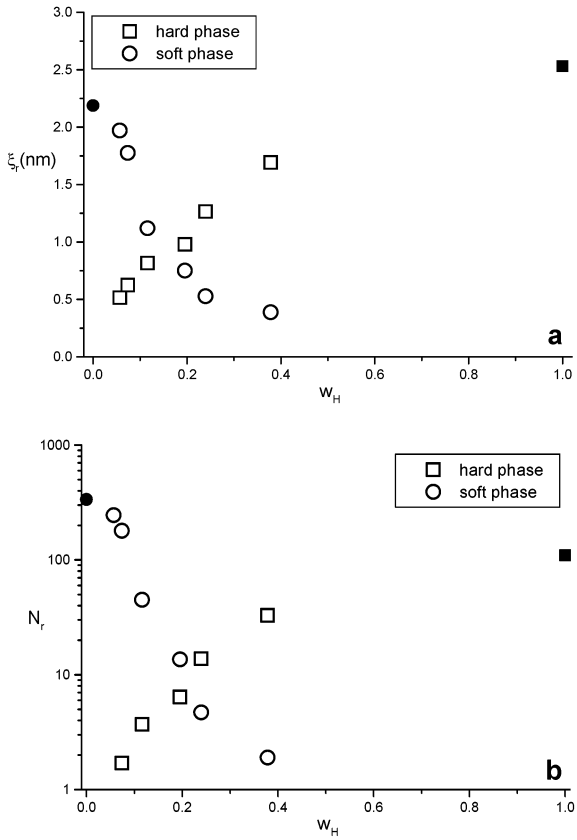

Figure 9. Dependence of the characteristic length ξ_r (a) and the cooperativity N_r (b) of the soft (○) and hard (□) transitions on the hydrogenated segment content w_H.

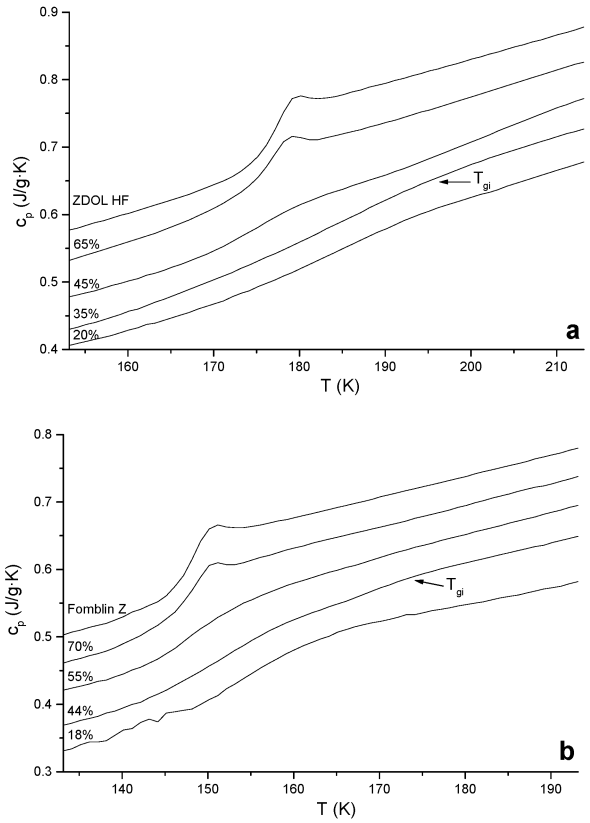

Figure 10. Heat capacity of the ZDOL HF/SiO_2 series (a) and of the Fomblin Z/SiO_2 series (b). The *Y* scale refers to bulk polymer data. Subsequent curves have been normalized to the organic phase weight content (indicated in the labels) and shifted successively by −0.05 J/(g K). The arrows highlight the weak glass transition associated with the interfacial layer (see text).

to Donth, we estimate δT from the empirical relation

$$\delta T = \Delta T/2.5 \tag{5}$$

where ΔT is the previously defined transition width.

The concept of CRR was introduced by Adam and Gibbs[38] as a subsystem which "can rearrange into another configuration independently of its environment". Equation 4 is so useful to give a comparative information about the size of cooperativity in amorphous systems with changing heterogeneity scale.

Figure 9a,b shows the behavior of the characteristic length ξ_r and of the cooperativity N_r, defined as the number of monomeric units inside an average CRR, for both transitions as a function of hydrogenated phase content. Correlations have been attempted between ξ_r and Angell's fragility[39] or the entanglement spacing;[40] for statistical copolymers, ξ_r has been reported to linearly vary between the values of corresponding homopolymers.[37,41]

In our copolymeric series, the cooperative size associated with both phases monotonically decreases, lowering the phase content. In this frame, an increased miscibility of the low molecular weight fluorinated segments seems not to be supported by the experimental results. The linear trend expected in a mixed system,[41] whose limiting values are represented by model homopolymers (solid markers in Figures 9), is completely overcome by a major effect of contraction of the characteristic length of the transition.

The size of the separated domains and the constraint effects, due to interfacial and morphological interplay, are known to exert an important part in the behavior of the glass transition. To investigate these effects, and to separate the role of the chemical bonding from the size confinement, a series of measurements were carried out by mixing fluorinated models with a calorimetrically inert porous SiO_2. Namely, a totally fluorinated unfunctionalized PFPE (Fomblin Z) and a fluorinated macromonomer bearing methylol chain ends (ZDOL HF) were adsorbed on different amounts of silica.

Parts a and b of Figure 10 show the heat capacity curves relative to the organic phase, ZDOL HF and Fomblin Z, respectively. SiO_2 heat capacity contribution has been measured in the same thermal range and subtracted from the experimental data. Finally, the resulting values have been normalized to the weight content of the organic phase.

A series of common features appear in both series:

(a) The hysteresis peak, clearly evident in the bulk fluorinated macromonomers, tends to disappear for an organic content below 50%. This qualitative behavior has been reported in block copolymers and blends as well as in polymers confined in nanometer sized pores.[42]

(b) The heat capacity jump Δc_p, normalized to the organic content (Figure 11), seems to reduce at low organic content. However, experimental values are scattered due to the increasing uncertainty in the correct step evaluation because of error propagation in the normalization process and of increasing broadening of the glass transition (see further).

(c) The midpoint temperature of the glass transition significantly increases by decreasing the fluorinated phase content. A preliminary study on the effect of a possible residue of solvent coming from the adsorption

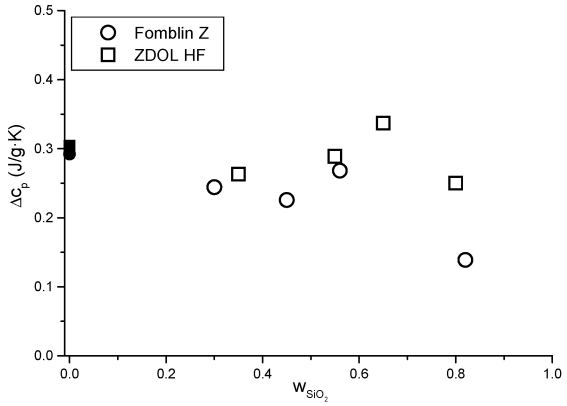

Figure 11. Measured Δc_p of the organic phase in the blends as a function of the silica weight content. Data are normalized to the organic content; solid markers indicate the bulk values.

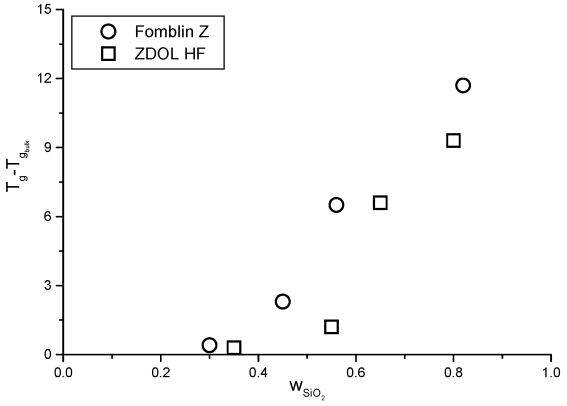

Figure 12. Difference between the glass transition temperature measured on the organic phase absorbed on silica and the bulk values plotted as a function of the weight content of silica.

procedure has shown that the expected decrease of the glass transition temperature is roughly in agreement with the Gordon−Taylor rule. This experimental disguise, if present, could not therefore explain the observed increase in T_g compared to bulk values.

The methylol chain ends of ZDOL HF moiety are expected to establish an effective hydrogen bond with the silica surface.[43] This general behavior has been observed for many surfaces containing polar active sites.[44] The effects on the glass transition of the reduced chain mobility in the interfacial region, due to different constraints, have been largely discussed for thin films on various substrates,[45−48] as well as for the natural constraints arising in the amorphous region in semicrystalline polymers[26,31,49] or in microphase-separated block copolymers.[9,33]

The role of hydrogen bonding on the observed dependence of glass transition on the filler content, i.e., on the surface/volume ratio, should be clarified by the investigation of the simpler system Fomblin Z/SiO_2 (Figure 10b). This perfluorinated, unfunctionalized, and apolar chain cannot have any kind of chemical bonding with the silica matrix unlike weak van der Waals interactions. Therefore, relevant effects on the phase transitions, if present, should be explained uniquely in terms of size or confinement effects.

Figure 12 reports, as a function of the weight content of silica, the difference between the T_g measured on the blends and the bulk value. For both polar and apolar

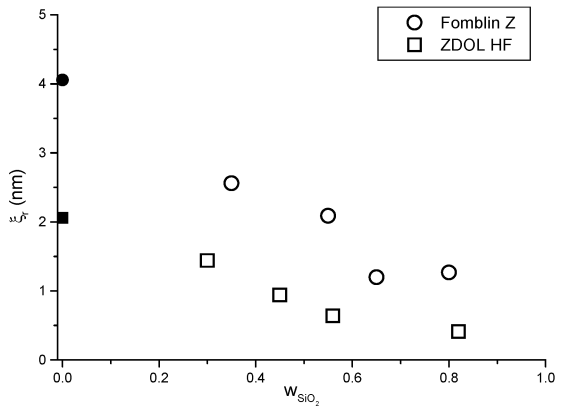

Figure 13. Dependence of the characteristic length ξ_r of Fomblin Z (□) and ZDOL HF (○) on the silica weight content. Solid markers represent bulk values.

fluorinated macromonomers the T_g increase exceeds the experimental error for an organic weight roughly less than 50%. Both series show a similar trend of T_g increase as a function of blend composition. These combined evidence suggests that the role of chemical interaction with surface seems to be marginal compared to confinement effects. A similar strong dependence of the glass transition temperature on the thickness is reported, for instance, in studies on supported[46] and freely standing[50] polymeric films thinner than a few hundred angstroms.[51]

Moreover, an accurate analysis of the DSC traces allows, in some samples, the identification of a weak glass transition some 20 deg higher than the main transition, in agreement with similar findings in PS/*o*-TP confined in controlled pore glasses.[42] According to the Park and McKenna interpretation, this second transition, indicated as T_{gi} in Figures 10, should be associated with the surface layer directly interacting with the silica surface.

Decreasing the total organic content, the two transitions apparently collapse into a unique broad transition: the increase of the experimental error due to the lower organic phase and the broadening connected to the nanosized confinement does not allow to further distinguish any separated transition.

(d) The glass transition is progressively broadened by decreasing the content of the organic phase. The broadening of the glass transition has been observed in several polymeric blends and has been generally associated with small scale compositional fluctuations.[52] This phenomenon is also a typical feature of many kinds of microsegregated systems associated with size and constraints on microdomains.[53]

In the two series of PFPE/SiO_2 mixtures, the characteristic length ξ_r associated with the CRR of the organic homophase, calculated from the experimental ΔT, shows a dependence on the organic content substantially unconnected to the bonding capability of the macromonomer to the hard inorganic phase (Figure 13).

This set of experimental evidence highlights the importance of the confinement effects on the phenomenology of the glass transitions of micro- or nanosegregated domains. The thermal behavior of a pure fluorinated phase confined on a solid surface shows the same features of a soft phase linked by a covalent bond to a hard microdomain.

The broadening of the glass transition, the disappearance of the hysteresis peak, and the apparent reduction

of the measured heat capacity step at T_g, lowering the domain dimension, should be related to the increasing contribution of the confinement effects deriving from the size of phase separation. The opposite sign of the T_g shift decreasing the phase content (positive for the soft phase, negative for the hard one) could be attributed to the opposite constraints on the chain mobility exerted in the phase boundaries. Previous results obtained on similar systems[9,17,54,55] were explained with the formation of mixed phases for very low molecular weight of the soft segment. The DSC analysis carried out in the current work indicates the growing contribution of the size effects on the glass transition behavior decreasing the soft segment length.

Conclusions

In a series of linear segmented polyurethanes constituted by a perfluorinated soft block of varying length and a diisocyanate hard segment without any chain extender, the heat capacity analysis as a function of temperature shows that two completely amorphous phases segregate whitin the whole compositional range. The variation of the molecular weight of the soft fluorinated spacers controls the size of the incompatible domains and determines the modification of the glass transition behavior for both phases. Comparing the glass transition parameters obtained on the investigated series with those measured on polymeric models of a fluorinated soft homophase and of a hydrogenated hard one, the hysteresis peak disappears, the glass transition broadens, and the measured heat capacity step at T_g reduces for both phases by decreasing the respective weight content in the polyurethane. Moreover, T_g shifts to higher temperatures for the soft phase and to lower temperatures for the hard one.

To clarify the reasons of these behaviors, two fluorinated macromonomers compositionally identical to the soft phase in the polyurethanes and with different chain ends (in order to change the nature of the interaction with the inorganic substrate) were absorbed on porous silica with a high specific surface area. Reducing the fluorinated phase content, the glass transitions were observed to shift to higher temperature and to broaden analogously to the behavior reported on the segregated soft phase of the polyurethane series, independent from the interaction of the macronomer with the silica surface.

Size effects, related to the changing mobility of confined chains, are so indicated as significantly contribute to the glass transition behavior of the segregated polyurethanes. A complete phase separation cannot be excluded even for amorphous polyurethanes constituted by very short, incompatible segments. Moreover, quantitative DSC can be a useful tool in the analysis of the segregation completeness as well as of the dimensional scale of the generated micro- or nanophases.

Acknowledgment. Solvay Solexis is acknowledged for permission to publish this work.

References and Notes

(1) Sauders, J. H.; Frisch, K. C. In *Polyurethanes Chemistry and Technology*; Interscience Publisher: New York, 1962; Part I, Chapter 6.
(2) Van Bogart, J. W. C.; Lilaonitkul, A.; Cooper, S. L. In *Morphology and Properties of Segmented Copolymers*; Advanced Chemical Series; American Chemical Society: Washington, DC, 1979; p 3.
(3) Meckel, D. C. W.; Goyert, W.; Wieder, W. In *Thermoplastic Elastomer*, 2nd ed.; Holden, G., Legge, N. R., Quirk, R., Schroeder, H. E., Eds.; Hanser: New York, 1996; Chapter 2.
(4) Koberstein, J. T.; Leung, L. M. *Macromolecules* **1992**, *25*, 6205.
(5) Wagener, K. B.; Matayabas, J. C., Jr. *Macromolecules* **1991**, *24*, 618.
(6) Leung, L. M.; Koberstein, J. T. *Macromolecules* **1986**, *19*, 706.
(7) Camberlin, Y.; Pascault, J. P. *J. Polym. Sci., Polym. Chem. Ed.* **1983**, *21*, 415.
(8) Brunette, C. M.; Hsu, S. L.; Rossman, M.; Macknight, W. J.; Schneider, N. S. *Polym. Eng. Sci.* **1981**, *21*, 668.
(9) Tonelli, C.; Bassi, M.; Ajroldi, G. *J. Polym. Sci., Polym. Phys. Ed.* **1999**, *37*, 1609.
(10) Koberstein, J. T.; Galmbos, A. F.; Leung, L. M. *Macromolecules* **1992**, *25*, 6195.
(11) Chen, T. K.; Shieh, T. S.; Chui, J. Y. *Macromolecules* **1998**, *31*, 1307.
(12) Chen, T. K.; Chui, J. Y.; Shieh, T. S. *Macromolecules* **1997**, *30*, 5068.
(13) Marchionni, G.; Ajroldi, G.; Pezzin, G. In *Comprehensive Polymer Science*; Aggarwal, S. L., Russo, S., Eds.; Pergamon Press: London, 1996; 2nd Suppl.
(14) Tonelli, C.; Trombetta, T.; Scicchitano, M.; Castiglioni, G. *J. Appl. Polym. Sci.* **1995**, *57*, 1031.
(15) Tonelli, C.; Trombetta, T.; Scicchitano, M.; Simeone, G. *J. Appl. Polym. Sci.* **1996**, *59*, 311.
(16) Tonelli, C.; Ajroldi, G. *J. Appl. Polym. Sci.* **2003**, *87*, 2279.
(17) Yoon, S. C.; Ratner, B. *Macromolecules* **1988**, *21*, 2401.
(18) Mathot, V. B. F. In *Calorimetry and Thermal Analysis of Polymers*; Mathot, V. B. F., Ed.; Carl Hanser Verlag: Munich, 1994.
(19) Marchionni, G.; Ajroldi, G.; Cinquina, P.; Tampellini, E.; Pezzin, G. *Polym. Eng. Sci.* **1990**, *30*, 829.
(20) Danusso, F.; Levi, M.; Gianotti, G.; Turri, S. *Macromol. Chem. Phys.* **1995**, *196*, 2855.
(21) Danusso, F.; Levi, M.; Gianotti, G.; Turri, S. *Polymer* **1993**, *34*, 3687.
(22) Staccione, A.; Ajroldi, G.; Marchionni, G.; Rebosio, L. *J. Polym. Sci., Part B: Polym. Phys.* **1997**, *35*, 2073.
(23) Gaur, U.; Wunderlich, B. *Macromolecules* **1980**, *13*, 1618.
(24) Morèse-Séguéla, B.; St-Jacques, M.; Renaud, J. M.; Prud'homme, J. *Macromolecules* **1980**, *13*, 100.
(25) Menczel, J.; Wunderlich, B. *J. Polym. Sci., Polym. Lett. Ed.* **1981**, *19*, 261.
(26) Cheng, S. Z. D.; Cao, M.-Y.; Wunderlich, B. *Macromolecules* **1986**, *19*, 1868.
(27) Lau, S.-F.; Pathak, J.; Wunderlich, B. *Macromolecules* **1982**, *15*, 1278.
(28) Fried, J. R.; Karasz, F. E.; MacKnight, W. J. *Macromolecules* **1978**, *11*, 150.
(29) Krause, S.; Iskandar, M.; Iqbal, M. *Macromolecules* **1982**, *15*, 105.
(30) Meyer, G. C.; Widmeier, J. M. *J. Polym. Sci., Polym. Phys. Ed.* **1982**, *20*, 389.
(31) Cheng, S. Z. D.; Wunderlich, B. *J. Polym. Sci., Polym. Phys. Ed.* **1986**, *24*, 595.
(32) ten Brinke, G.; Karasz, F. E.; Ellis, T. S. *Macromolecules* **1983**, *16*, 244.
(33) Wang, B.; Krause, S. *Macromolecules* **1987**, *20*, 2201.
(34) Delucchi, M.; Turri, S.; Barbucci, A.; Bassi, M.; Novelli, S.; Cerisola, G. *J. Polym. Sci., Part B: Polym. Phys.* **2002**, *40*, 52.
(35) Camberlin, Y.; Pascault, J. P. *J. Polym. Sci., Polym. Phys. Ed.* **1984**, *22*, 1835.
(36) Donth, E. *J. Non-Cryst. Solids* **1982**, *53*, 325.
(37) Donth, E. *J. Polym. Sci., Part B: Polym. Phys.* **1996**, *34*, 2881.
(38) Adam, G.; Gibbs, H. J. *J. Chem. Phys.* **1965**, *43*, 139.
(39) Hempel, E.; Hempel, G.; Hensel, A.; Schick, C.; Donth, E. *J. Phys. Chem. B* **2000**, *104*, 2460.
(40) Donth, E.; Beiner, M.; Reissig, S.; Korus, J.; Garwe, F.; Vieweg, S.; Kahle, S.; Hempel, E.; Schröter, K. *Macromolecules* **1996**, *29*, 6589.
(41) Kahle, S.; Korus, J.; Hempel, E.; Unger, R.; Höring, S.; Schröter, K.; Donth, E. *Macromolecules* **1997**, *30*, 7214.
(42) Park, J.-Y.; McKenna, G. B. *Phys. Rev. B* **2000**, *61*, 6667.
(43) Tonelli, C.; Gavezotti, P.; Strepparola, E. *J. Fluorine Chem.* **1999**, *95*, 51.
(44) Tyndall, G. W.; Waltman, R. J.; Poker, D. J. *Langmuir* **1998**, *14*, 7527.

(45) Keddie, J. L.; Jones, R. A. L.; Cory, R. A. *Faraday Discuss.* **1994**, *98*, 219.
(46) DeMaggio, G. B.; Frieze, W. E.; Gidley, D. W.; Zhu, M.; Hristov, H. A.; Yee, A. F. *Phys. Rev. Lett.* **1997**, *78*, 1524.
(47) Tsui, O. K. C.; Russel, T. P. *Macromolecules* **2001**, *34*, 5535.
(48) Fryer, D. S.; Peters, R. D.; Kim, E. J.; Tomaszewski, J. E.; de Pablo, J. J.; Nealey, P. F. *Macromolecules* **2001**, *34*, 5627.
(49) Dobbertin, J.; Hensel, A.; Stick, C. *J. Therm. Anal.* **1996**, *47*, 1027.
(50) Forrest, J. A.; Dalnoki-Verres, K.; Dutcher, J. R. *Phys. Rev. Lett.* **1996**, *77*, 2002.
(51) Kim, J. H.; Jang, J.; Zin, W.-C. *Langmuir* **2001**, *17*, 2703.
(52) Hale, A.; Harvey, H. E. In *Thermal Characterization of Polymeric Materials*, 2nd ed.; Turi, E. A., Ed.; Academic Press: New York, 1997; Vol. 1, p 757.
(53) Wunderlich, B. *Thermal Analysis*; Academic Press: San Diego, 1990; p 296.
(54) Simeone, G.; Turri, S.; Scicchitano, M.; Tonelli, C. *Makromol. Chem.* **1996**, *236*, 111.
(55) Priola, A.; Bongiovanni, R.; Malucelli, G.; Pollicino, A.; Tonelli, C.; Simeone, G. *Macromol. Chem. Phys.* **1997**, *198*, 1893.

MA034674G